ELSEVIER

Polymer 40 (1999) 1985–1992

polymer

Effect of acrylonitrile content on the delamination toughness of PC/SAN microlayers

T. Ebeling, A. Hiltner*, E. Baer

Department of Macromolecular Science and Center for Applied Polymer Research, Cleveland, OH 44106-7202, USA

Received 20 March 1998; accepted 20 May 1998

Abstract

The effect of acrylonitrile (AN) content on the adhesion of poly(styrene-co-acrylonitrile) (SAN) to polycarbonate (PC) was examined by measuring the delamination toughness of PC/SAN microlayers in the T-peel test. Experiments were carried out on microlayers with thin SAN layers, to ensure that delamination would occur predominantly by an interfacial mechanism, and with PC layers that were thick enough to prevent the delamination crack from tearing through the PC. Layer thicknesses of approximately 4.5 μm/0.5 μm (PC/SAN) gave satisfactory results. A broad maximum in the interfacial toughness occurred at about 20% AN. When microlayers with thicker SAN layers were tested, only SAN compositions with 15–25% AN crazed. This increased the delamination toughness and greatly exaggerated the maximum at 20% AN. Crazing only occurred if the interfacial toughness of PC-SAN exceeded the SAN crazing condition. When the crazing condition, which increased linearly with AN content, was overlayed with the interfacial toughness, the intersections correctly predicted the AN content for transitions in failure mode.

Keywords: Polycarbonate; Poly(styrene-co-acrylonitrile); Microlayers; Delamination toughness; SAN acrylonitrile content

1. Introduction

The commercial importance of PC/ABS blends, e.g. in automotive applications, and the possibility for varying the adhesion of polycarbonate (PC) to poly(styrene-co-acrylonitrile) (SAN) by changing the acrylonitrile (AN) content constitute the major impetus for previous studies of PC-SAN adhesion [1–5]. It has been recognized for some time that normal test methods can give values for the interfacial toughness of immiscible polymers that are unexpectedly high [6–8]. Often, the high values are caused by crazing in the polymer with the lower craze resistance. It appears likely that crazing was a factor in some previous measurements of PC-SAN interfacial toughness and the reported values may therefore be too high.

The flexibility of the microlayer process and the control afforded of layer thickness make microlayers attractive for studying polymer–polymer adhesion. From previous studies that describe the delamination mode and delamination toughness of PC/SAN microlayers, conditions of layer thickness [9,10] and peel rate [10,11] have been identified under which crazing does not occur and the peel force is a measure of interfacial toughness. These studies are now extended to consider the effects of AN content on delamination mode and delamination toughness.

2. Experimental

Coextruded microlayer sheets were either supplied by The Dow Chemical Company, Midland, MI, or coextruded using the CWRU layer multiplying process described previously [12]. In both cases, the PC was Merlon M-40 (Mobay) with a molecular weight of 28 000–30 000 reported by the manufacturer. The SAN resins used in the CWRU process are described in Table 1. The molecular weight of the SAN resins was determined by GPC relative to PS standards with the appropriate correction [13]. The AN content provided by the manufacturer was confirmed by FTIR to be within 1%.

The SAN resins were tested for low molecular weight oligomers by measuring the change in the glass transition temperature after reprecipitation [14]. The SAN was dissolved in acetone at a concentration of 3 g dl^{-1}, precipitated in isopropanol, and dried in vacuum at 90°C for 24 h. The glass transition was obtained by differential scanning calorimetry using the Rheometrics DSC Plus with a heating rate of 20°C min^{-1}. The glass transition temperature was taken from the second heating thermogram. The oligomer content

* Corresponding author.

0032-3861/99/$ - see front matter
PII: S0032-3861(98)00416-9

Table 1
Composition of styrene–acrylonitrile copolymers

AN content (%)	M_w (PDI)	Source
0.0	567 000 (1.68) [a]	Dow (Styron 685)
5.5	170 000 [b]	Dow
8.5	170 000 [b]	Dow
16.0	170 000 [b]	Dow
20.0	171 000 (1.80) [a]	Dow (Tyril 990)
25.0	193 000 (1.91) [a]	Dow (Tyril 1000B)
30.0	151 000 (1.88) [a]	Dow (Tyril 880B)
34.0	134 000 (2.40) [a]	GE

[a] M_w determined by GPC relative to PS standard
[b] M_w provided by supplier

was estimated from the glass transition temperature using the Fox equation with −56.0°C as the T_g of the oligomer and 116.0°C as the T_g of oligomer-free SAN with 25% AN [14]. The amount of oligomer varied from 1.4 to 1.9%, consistent with previous findings on commercial SAN resins [4,14].

The oligomers were removed from about 1 kg of Tyril 1000B (25% AN) using the same procedure, and microlayers were prepared from this material. The as-received Tyril 1000B had a T_g of 111.8°C, indicating an oligomer content of about 1.4%. The reprecipitated resin had a T_g of 115.3°C, indicating a reduction in oligomer content to about 0.2%. In microlayers, the T_g of as-received Tyril 1000B increased from 111.8 to 115.0°C (0.2% oligomer). A similar shift in the T_g of SAN in PC/SAN blends was attributed to diffusion of SAN oligomers into the PC [4,14]. In contrast, the T_g of the reprecipitated Tyril 1000B in microlayers shifted slightly from 115.3 to 116.0°C (<0.1% oligomer).

Microlayer sheets, 1–2 mm in thickness, consisting of alternating layers of PC and SAN were coextruded using the CWRU layer multiplying process [12]. The number of layers and the extruder feed ratios were varied to produce microlayers with different compositions and layer thicknesses. Processing focused on microlayers with thin SAN layers, to ensure that delamination would occur predominantly by an interfacial mechanism, and with PC layers that were thick enough to prevent the delamination crack from tearing through the PC [9,10]. Layer thicknesses of approximately 4.5 μm/0.5 μm (PC/SAN) gave satisfactory results. Some microlayers with thicker SAN layers were prepared to examine the effects of layer thickness. Microlayers are identified by the average layer thicknesses which were calculated from the measured bulk thickness, the total number of layers and the feed ratio.

Additional PC/SAN microlayers were supplied by The Dow Chemical Company in the form of coextruded sheets about 1 mm thick. These materials were described in previous studies [15,16]; they contained from 49 to 776 alternating layers of PC and SAN with the outermost layers being PC. Two of the SAN resins used in the Dow microlayers were also used in the CWRU process: Tyril 867B (now Tyril 1000B) with 25% AN and Tyril 880B with 30% AN. Microlayers of SAN with 5.5% AN (194 layers), 8.5% AN (194 layers) and 16% AN (392 and 776 layers) were also provided by Dow. The compositions and layer thicknesses of all the microlayers are summarized in Table 2.

Table 2
Microlayer thicknesses and delamination mode and toughness

AN content [a] (%)	Layer thickness (PC/SAN) (μm/μm)	Delamination mode	Delamination toughness ($J\ m^{-2}$)
0.0 (C)	4.5/0.5	Interfacial	32 ± 3
0.0 (C)	4.8/1.6	Interfacial	37 ± 7
0.0 (C)	4.7/4.7	Interfacial	43 ± 6
0.0 (C)	2.0/6.0	Interfacial	48 ± 7
5.5 (D)	8.3/5.5	Interfacial	54 ± 4
5.5 (D) [b]	8.3/5.5	Interfacial	50 ± 3
8.5 (D)	8.2/3.5	Interfacial	53 ± 5
8.5 (D) [b]	8.2/3.5	Interfacial	48 ± 3
16.0 (D)	2.7/1.8	Crazing	160 ± 10
16.0 (D) [b]	2.7/1.8	Interfacial	62 ± 5
20.0 (C)	4.5/0.5	Interfacial	96 ± 6
20.0 (C)	6.0/2.0	Crazing	150 ± 20
20.0 (C)	3.9/3.9	Crazing	270 ± 40
20.0 (C)	2.0/5.9	Crazing	540 ± 70
25.0 (D)	9.1/0.2	Interfacial	94 ± 5
25.0 (D)	15.0/0.5	Interfacial	95 ± 3
25.0 (D)	14.0/0.7	Interfacial	90 ± 10
25.0 (D)	5.0/0.5	Interfacial	98 ± 6
25.0 (D)	4.2/0.5	Interfacial	88 ± 8
25.0 (C)	4.5/0.5	Interfacial	90 ± 8
25.0 (D)	2.5/0.5	Interfacial	92 ± 6
25.0 (D)	8.1/1.6	Crazing	135 ± 3
25.0 (C)	5.4/1.8	Crazing	180 ± 25
25.0 (D)	9.2/2.8	Crazing	165 ± 15
25.0 (D)	8.2/4.2	Crazing	180 ± 10
25.0 (C)	4.5/4.5	Crazing	240 ± 40
25.0 (D)	6.8/5.6	Crazing	220 ± 20
25.0 (C)	2.0/6.0	Crazing	220 ± 60
25.0 (D)	5.0/7.5	Crazing	300 ± 40
25.0 (D)	34.0/18.0	Crazing	320 ± 115
30.0 (D)	4.5/0.5	Interfacial	82 ± 6
30.0 (D)	8.1/2.7	Interfacial	84 ± 5
30.0 (D)	2.8/2.8	Interfacial	75 ± 8
30.0 (D)	4.3/4.3	Interfacial	98 ± 10

[a] (C), extruded at CWRU; (D), extruded at Dow
[b] Peeled at 0.002 mm min^{-1}

Delamination was carried out with the T-peel test (ASTM D 1876). Specimens 15–25 mm wide were notched by pushing a fresh razor blade into the midplane of the sheet. The notch was examined with an optical microscope to ensure that the crack started along a single layer. Specimens were peeled at room temperature at a rate of 2.0 mm min^{-1} unless otherwise indicated. In a few cases, microlayers with thicker SAN layers were peeled at a lower rate to achieve interfacial delamination [10,11]. Conformation of beam arm curvature in the T-peel test to Kendall's elastic prediction [17] confirmed that the beam arms deformed elastically, and therefore the critical load in the T-peel test measured resistance to crack propagation including the contribution of damage at the crack tip. The observation that the beam arms returned to their original positions upon removal of

the load further confirmed the absence of plastic deformation in the beam arms.

Some tests were interrupted and the crack tip region was sectioned perpendicular to the plane of the crack with a low speed diamond saw (Isomet, Buehler Ltd., Lake Bloff, IL). The sections were polished on a metallurgical wheel with wet sandpaper and alumina oxide aqueous suspensions and photographed in a transmission optical microscope. Sections of the fracture surfaces were coated with 90 Å of gold for examination in a JEOL JSM 840A scanning electron microscope. Uncoated fracture surfaces were analyzed with the Nicolet 800 FTIR spectrometer in the ATR mode with a germanium 60/60 crystal to determine the surface composition.

A 1 mm radius semi-circular notch was machined midway along one edge of a rectangular specimen, 120 mm × 20 mm, cut from an approximately 2.0 mm thick compression molded plaque of SAN. The notched bars were pulled at a crosshead speed of 0.1 mm min^{-1} with an initial grip separation of 100 mm. The growth of crazes in the triaxial stress state at the notch root was monitored with a video camera equipped with a traveling optical microscope. The published solution for the elastic stress field in front of a semi-circular edge notch was used to analyze the craze zone [18].

3. Results and discussion

3.1. Interfacial delamination of thin SAN layers

Typical normalized peel curves are illustrated in Fig. 1 for PC/SAN microlayers with AN content ranging from 0 to 30%. The load initially increased while the crack remained stationary and the beam arms bent into the T-peel configuration. When the peel toughness was achieved, the crack propagated continuously at a relatively constant load (P_{cr})

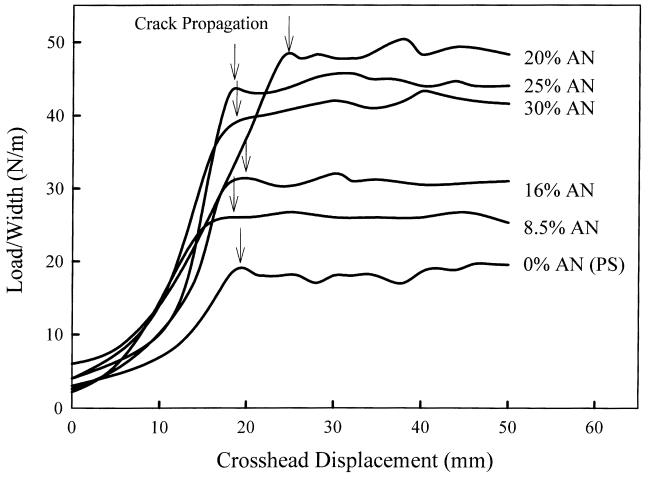

Fig. 1. Normalized peel curves of PC/SAN microlayers with layer thicknesses of approximately 4.5 μm/0.5 μm (PC/SAN). Arrows indicate the beginning of crack propagation.

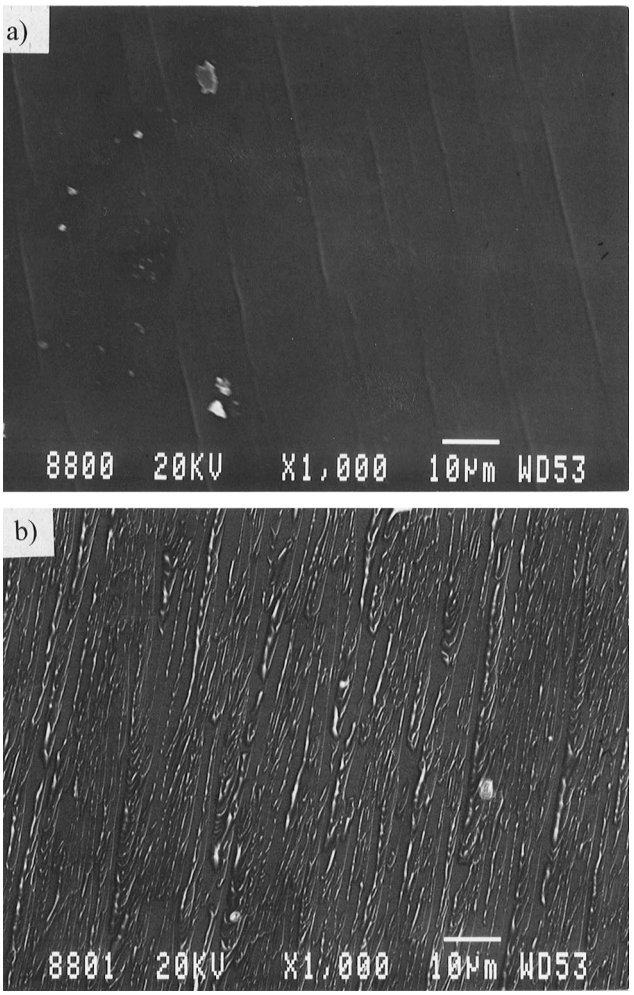

Fig. 2. Scanning electron micrographs of matching peel fracture surfaces of PC/SAN (4.5 μm/0.5 μm) with 30% AN: (a) the PC surface; and (b) the SAN surface. The crack propagated from left to right.

from which the delamination toughness was calculated as $G = 2P_{cr}/W$ for a specimen of width W. From Fig. 1, the delamination toughness was lowest when the AN content was 0% (PC/PS microlayer) and increased to a maximum for the SAN with 20% AN.

Failure by interfacial delamination was verified before the peel toughness was used as a measure of interfacial toughness. Methods of characterization included examination of the crack tip of partially peeled specimens to establish that the crack propagated along a single interface without crazing in the SAN layer, and analysis of the fracture surfaces by infrared spectroscopy to confirm that one surface was styrenic (PS or SAN) and the other surface was PC. In the SEM, interfacial failure surfaces were featureless at low magnification; however, at higher magnification they showed the micron scale features that typically accompany interfacial delamination of PC/SAN microlayers [9–11]. As exemplified by the fracture surfaces in Fig. 2, the smooth PC surface contained a few chunks of SAN and the matching SAN surface exhibited wrinkles and occasional holes where the chunks were pulled out. However, the damage

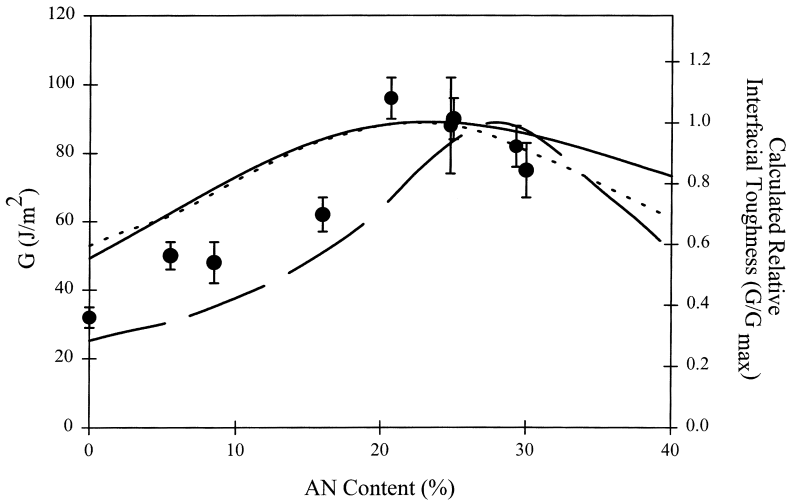

Fig. 3. Comparison of the measured interfacial toughness with predictions based on the interaction parameter χ: ——, from component monomers [3]; - - -, from low molecular weight PC [4]; — — —, from copolycarbonates [4].

associated with these features did not contribute measurably to the delamination toughness [9–11].

The interfacial toughness, taken as the delamination toughness of microlayers that failed by interfacial delamination, is plotted as a function of increasing AN content in Fig. 3. The plot includes data from samples prepared by the CWRU process and by Dow from the same SAN resins (25% and 30% SAN). Peel measurements on microlayers prepared by the two processes gave the same results. In addition, removing the oligomers from the SAN did not significantly affect the interfacial toughness. Although the effect of AN content was not dramatic, there was a broad maximum in the interfacial toughness. The toughness approximately tripled as the AN content increased from 0 and 20%, then it gradually decreased as the AN content increased further to 30%. The magnitude of the interfacial toughness obtained by peeling microlayers was comparable to reported values, particularly those where it was explicitly indicated that crazing did not increase the toughness [3,7]. The maximum at 20% AN was also consistent with a number of previous studies [1–4,14]. Studies where crazing may have contributed to the measured adhesive strength showed a much higher peak.

On a molecular scale, interfacial adhesion requires chain segments to diffuse across the interface. Based on evidence that the depth of segmental diffusion is inversely proportional to the interaction parameter χ [3], the simplest approach is to assume that G is proportional to χ^{-1}. Included in Fig. 3 are several predictions of the relative interfacial toughness based on the interaction parameter. The calculations rely on estimated values of the interaction parameter because the polymers are immiscible at all temperatures and conventional cloud point measurements can not be used. One approach estimates χ from Flory's equation for the interaction parameter of a homopolymer–copolymer pair using values of the interaction parameters for the component monomers [3]. Alternative calculations are based on miscibility of low molecular weight PC and SAN, and on miscibility of co-polycarbonates with SAN [4]. The magnitude of the AN effect on interfacial toughness correlates best with predictions based on co-polycarbonates; however, the AN content for maximum adhesion is predicted somewhat better by the other estimates.

3.2. Delamination of thick SAN layers

The delamination toughness of microlayers with approximately 4 μm thick SAN layers is compared with the interfacial toughness in Fig. 4. The increase in SAN layer thickness had only a slight effect on the delamination

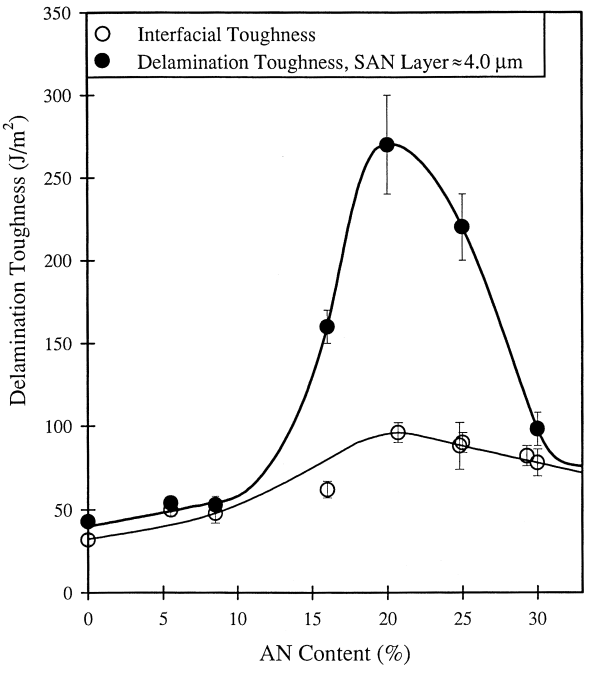

Fig. 4. Delamination toughness of microlayers with SAN layers approximately 4 μm thick compared with the interfacial toughness.

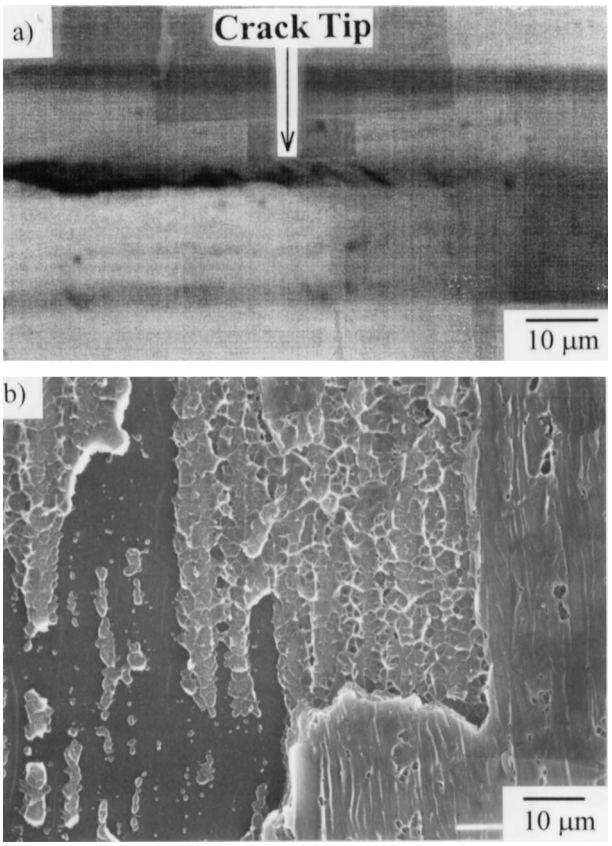

Fig. 5. Peel of PC/SAN (8.2 μm/4.2 μm) with 25% AN: (a) the crack tip; and (b) the fracture surface. The crack propagated from left to right.

toughness of SANs with either low or high AN content. Fractography confirmed that failure of these compositions occurred by interfacial delamination regardless of the SAN layer thickness. This was in sharp contrast to SANs with 15–25% AN where the delamination toughness of thicker SAN layers considerably exceeded the interfacial toughness. Examination of a partially peeled specimen revealed crazing ahead of the crack tip in a SAN layer with 25% AN (Fig. 5a). Fractographic examination confirmed that the delamination crack alternately propagated through crazes in the SAN layer and along the PC-SAN interface. The fracture surface in Fig. 5b provided evidence that as the crack moved from left to right, it propagated along one interface, where the smooth surface littered with chunks of material was typical of the PC surface (compare with Fig. 2a), then through a craze, as seen by the cavitated and fibrilated material, and finally along the other interface, where holes remained in the wrinkled SAN surface (compare with Fig. 2b).

Crazing ahead of the crack tip effectively reduced the stress concentration at the interface and increased the delamination toughness. Fig. 6 illustrates this effect with a three-dimensional plot of delamination toughness as a function of SAN layer thickness and AN content. The data plotted in Fig. 6 are included in Table 2. For those compositions that crazed, the amount of crazing and hence the delamination toughness increased with the SAN layer thickness. The strong dependence of delamination toughness on SAN thickness clarified why some literature reports describe a much more dramatic dependence of interfacial adhesion on AN content than is presented in Fig. 3. Unless the thickness of the SAN layer was a micron or less, crazing accompanied delamination of SAN compositions in the intermediate AN range. The crazing contribution exaggerated the interfacial strength of these SAN compositions in comparison to SANs with low or high AN content which always failed by interfacial delamination.

More importantly, the results provided evidence of transitional behavior in the delamination mechanism with variation of the AN content. A transition from interfacial

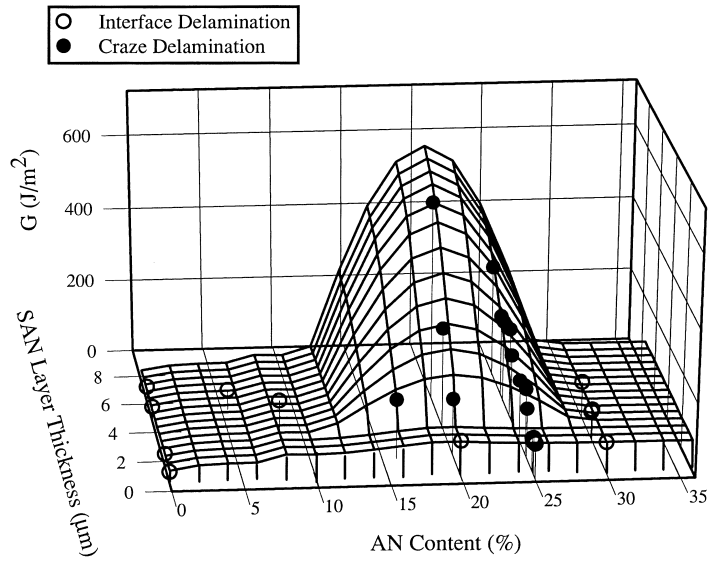

Fig. 6. Three-dimensional plot of delamination toughness as a function of AN content and SAN layer thickness: ○, interfacial delamination; ●, craze delamination.

failure to crazing could occur if the adhesive strength of SAN to PC exceeded the SAN crazing condition. Both characteristics are expected to depend on AN content; however, they will not necessarily depend on AN content in the same way. The interaction parameter with PC determines the interfacial toughness; in contrast, the properties of SAN, such as entanglement density, surface energy and glass transition temperature (as well as strain rate and temperature), control the crazing condition.

3.3. Effect of AN content on SAN crazing

Crazing of SAN under a triaxial stress state was examined by loading a single edge notch specimen in tension according to the methodology described previously [18]. The moderate stress intensification and relatively smooth stress gradients at the semicircular notch minimized the tendency for premature brittle fracture. Furthermore, an exact numerical solution of the elastic stress field distribution was available. Upon loading, the first damage observed was discontinuous surface crazes that followed curved trajectories. At a slightly higher remote stress, internal crazes initiated at the notch surface and grew within the specimen along linear trajectories. The zone defined by the tips of the internal notch crazes was initially crescent-shaped, but it acquired a more triangular shape as the remote stress increased.

The remote stress at which internal crazes were first observed increased with the AN content of the SAN. This is evident in Fig. 7 where craze zones of PS and SANs with 20%, 25% and 30% AN are compared at about the same remote stress. In PS, the zone was very large and strongly deviated from the initial crescent shape. The zone of SAN with 20% AN was smaller and closer to a crescent shape. As the AN content increased, the zone gradually decreased in size: the small zone of the 25% AN resin demonstrated the initial crescent shape, and the 30% AN resin revealed only initiation of a few short internal crazes. Qualitatively, this indicated that the resistance to crazing increased with the AN content.

To analyze the craze zone, the bulk glassy material was treated as a linear elastic solid. Because the crazes were load-bearing, it was assumed that they did not affect the stress distribution significantly when the craze zone was small. The principal stresses σ_1 and σ_2 were obtained as described previously [18] and in the case of plane strain $\sigma_3 = \nu(\sigma_1 + \sigma_2)$. A value of Poisson's ratio $\nu = 0.35$ was used to obtain the mean stress $\sigma_m = (\sigma_1 + \sigma_2 + \sigma_3)/3$. In accordance with previous results, the positions of the craze tips fit a constant mean stress condition which defined the critical mean stress for internal craze growth σ_{mc} [11,18]. By restricting the analysis to small craze zones, i.e. those formed at remote loads not more than 5 MPa above the craze initiation load, σ_{mc} deviated by less than $\pm 5\%$ from the mean. At higher remote loads, stress redistribution caused the craze zone to take on a triangular shape and the position of the craze tips no longer conformed with the constant σ_{mc} condition. The critical mean stress for crazing is plotted in Fig. 8 as a function of the AN content where each point represents an average of at least four tests. The critical mean stress was lowest for PS and increased

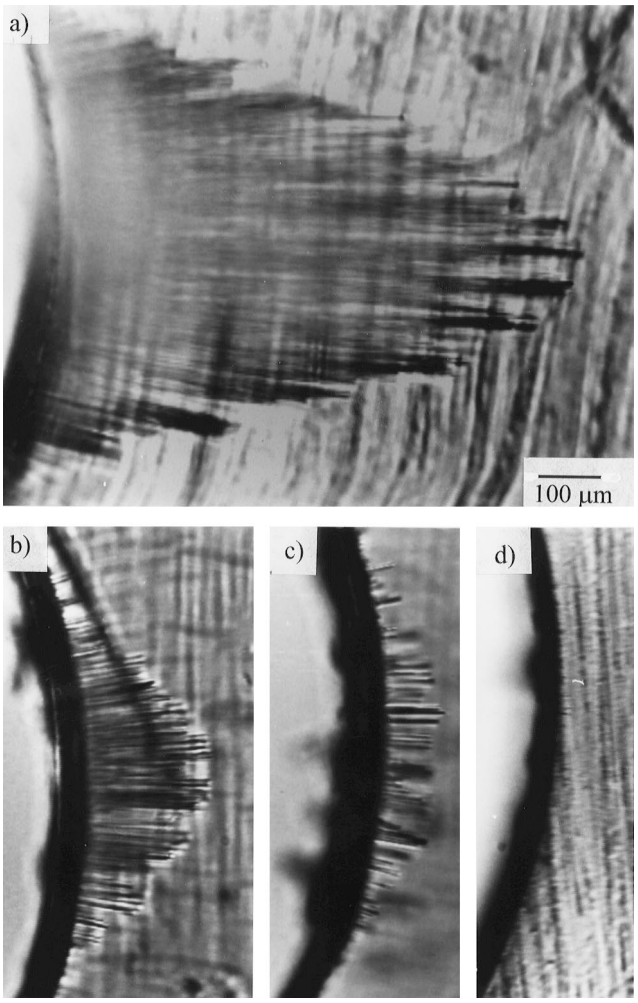

Fig. 7. Optical micrographs of the craze zone at a semicircular edge notch, all at a remote stress of about 30 MPa: (a) PS; (b) SAN with 20% AN; (c) SAN with 25% AN; and (d) SAN with 34% AN.

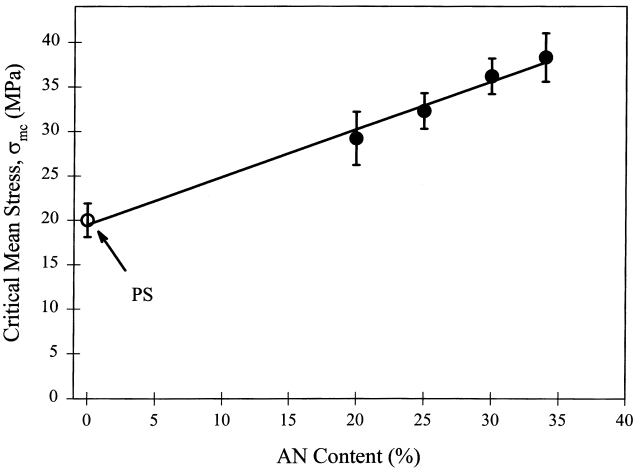

Fig. 8. Critical mean stress σ_{mc} as a function of AN content.

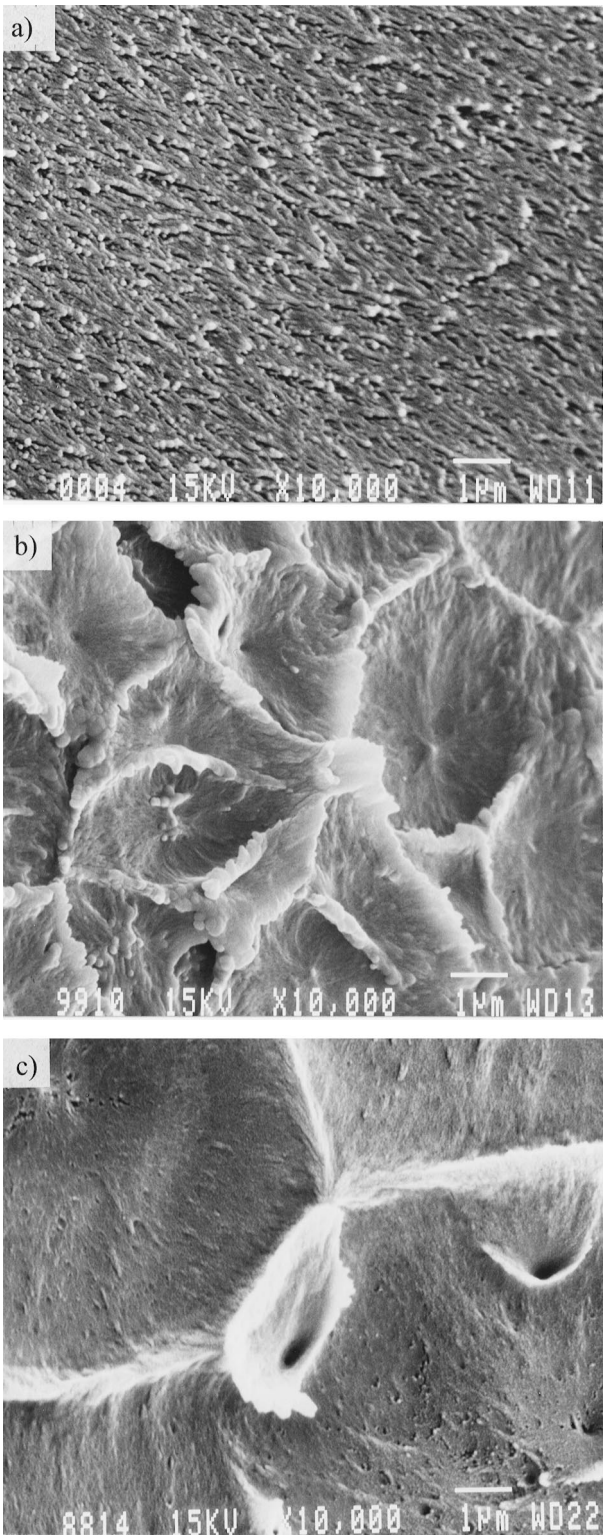

Fig. 9. Scanning electron micrographs comparing the craze fibril morphology on the fracture surface: (a) PS; (b) SAN with 25% AN; and (c) SAN with 30% AN.

linearly with the AN content until the critical mean stress of the 34% AN resin was almost twice that of PS. The trend correlated with increased entanglement density which increased the craze resistance [19].

Catastrophic fracture through the pre-existing craze zone occurred at about the same extension for all the resins, except for the 34% AN resin which fractured at a lower strain. Because craze resistance increased with AN content, the length of the pre-existing craze zone when fracture initiated shortened as the AN content increased. The length was 2.2, 1.1, 0.8, 0.7 and 0.1 mm for 0, 20, 25, 30, and 34% AN, respectively. Nevertheless, all the fracture surfaces contained the three regions typical of craze fracture of brittle, glassy polymers: textured and smooth regions where the crack propagated through the pre-existing craze, and a banded hackle region. The micrographs in Fig. 9 compare the textured region produced by cavitation and crack propagation along the fibril mid-plane. The PS surface in Fig. 9a showed dense craze fibrils characteristic of craze fracture in this polymer. In contrast, the SAN with 25% AN exhibited a porous texture that consisted of thick fractured fibrils and membrane-like connections between fractured fibrils (Fig. 9b). Increasing the AN content to 30% resulted in larger pores with a few very thick craze fibrils (Fig. 9c). Although craze fibrils recoil and change dimensions upon fracture, the micrographs clearly showed an increase in fibril diameter and decrease in fibril density with increasing AN content. This trend reflected the higher surface energy caused by a higher entanglement density [19]. The texture of craze fibril fracture in bulk SAN closely resembled the fracture features of craze delamination (Fig. 9b compared with Fig. 5b). Craze delamination can be considered as craze fracture in a confined geometry. If the fundamental processes of fibril formation and fracture are the same, it follows that the condition for craze growth in bulk resin can also apply to craze delamination in the T-peel test.

3.4. Relationship between bulk crazing and delamination mode

The absence of craze delamination in SAN microlayers with either high or low AN content can be understood by considering the competition between crazing and interfacial failure. If the critical stress condition for SAN crazing, which increases linearly with AN content, is overlayed with the interfacial toughness, transitions in the failure mode should occur where the craze line crosses the interfacial failure curve. To make this comparison, the craze condition in the T-peel test (G_{craze}) is derived from the craze condition measured in notched tension experiments (σ_{mc}). This requires consideration of differences in test rate and stress state of the two methods. According to the previous study of rate effects in these systems [11], a factor of 200 in nominal test rate produces equivalent local strain rates, i.e. T-peel tests at 2.0 mm min^{-1} should be compared with σ_{mc} measurements at 0.01 mm min^{-1}. From the rate dependence of σ_{mc}, determinations made at 0.1 mm min^{-1} are multiplied by 0.9 to obtain σ_{mc} at 0.01 mm min^{-1}. To compensate for the difference in stress state, proportionality is assumed, i.e. $G_{craze} = K\sigma_{mc}$. The value of $K = 2.44$ obtained previously gives the craze condition for peel

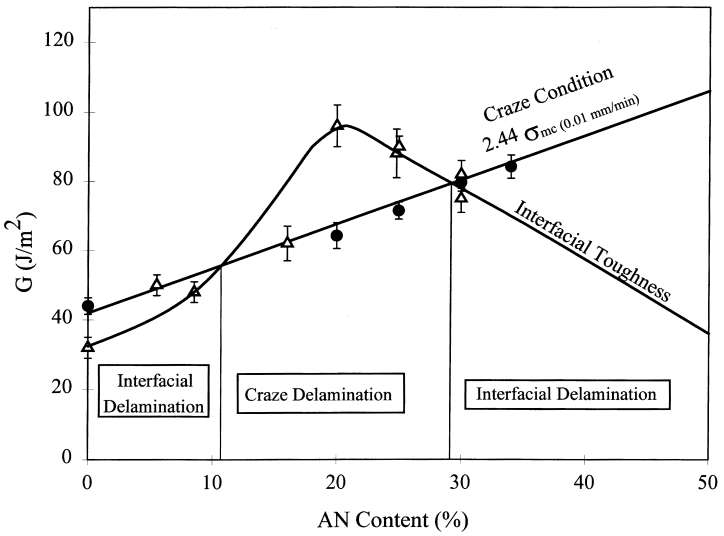

Fig. 10. Comparison of interfacial toughness with the craze condition as a function of AN content: △, interfacial toughness; ●, the craze condition.

plotted in Fig. 10. In composition ranges where the interfacial toughness is lower than G_{craze}, the failure mode is interfacial and the measured toughness is essentially independent of layer thickness. On the other hand, for intermediate SAN compositions with more than 10%AN but less than 30% AN, G_{craze} is lower than the interfacial toughness. For these, the development of a craze zone and subsequent fracture through the craze zone increase the measured delamination toughness considerably.

In summary, peel tests of PC/SAN microlayers measure interfacial toughness if the SAN layers are thin enough to suppress crazing and the PC layers are thick enough to prevent crack jumps from one interface to the next. The results of peel tests confirm an optimum AN content for maximum PC-SAN adhesion in the range of about 20% AN. The relatively small variation in interfacial toughness with AN content, about a factor of 3, has a dramatic effect when the SAN layers are thick enough to craze. If the craze initiation condition is lower than the interfacial toughness, formation of a craze zone increases the delamination toughness dramatically.

Acknowledgements

This work was generously supported by the Army Research Office (grant DAAL03-92-G-0241) and the National Science Foundation (grant DMR97-05696).

References

[1] Keitz JD, Barlow JW, Paul DR. J Appl Polym Sci 1984;29:3131.
[2] Janarthanan V, Stein RS, Garrett PD. J Polym Sci: B: Polym Phys 1993;31:1995.
[3] Willett JL, Wool RP. Macromolecules 1993;26:5336.
[4] Callaghan TA, Takakuwa K, Paul DR, Padwa AR. Polymer 1993; 34:3796.
[5] Watkins VH, Hobbs SY. Polymer 1993;34:3955.
[6] Robertson RE. J Adhesion 1972;4:1.
[7] Brown HR. J Mater Sci 1990;25:2791.
[8] Creton C, Kramer EJ, Hui C-Y, Brown HR. Macromolecules 1992;25:3075.
[9] Ebeling T, Hiltner A, Baer E. J Appl Polym Sci, in press.
[10] Hiltner A, Ebeling E, Shah A, Mueller C, Baer E. In: Lohse DJ, Russell TP, Sperling LH, editors. Interfacial aspects of multicomponent polymer materials. New York:Plenum, 1997:95–106.
[11] Ebeling T, Hiltner A, Baer E. Polymer, in press.
[12] Mueller CD, Nazarenko S, Ebeling T, Schuman TL, Hiltner A, Baer E. Polym Eng Sci 1997;37:355.
[13] Mendelson RA. In: Provder T, editor. Detection and data analysis in size exclusion chromatography. Washington, DC: ACS, 1987:263–280.
[14] Guest MJ, Daly JH. Eur Polym J198925 :985.
[15] Im J, Baer E, Hiltner A. In: Baer E, Moet A, editors. High performance polymers. Munich: Hanser, 1991:175–198.
[16] Haderski D, Sung K, Im J, Hiltner A, Baer E. J Appl Polym Sci 1994;52:121.
[17] Kendall K. J Adhesion 1973;5:105.
[18] Shin E, Hiltner A, Baer E. J Appl Polym Sci 1992;46:213.
[19] Kramer EJ, Berger LL. In: Kausch HH, editor. Advances in polymer science 91/92. Berlin: Springer, 1990:1–68.